REPORT DOCUMENTATION PAGE

Form Approved OMB NO. 0704-0188

1. REPORT DATE (DD-MM-YYYY)	2. REPORT TYPE	3. DATES COVERED (From - To)
22-11-2013	Final Report	1-Sep-2010 - 31-Aug-2013

4. TITLE AND SUBTITLE
Charge Density Engineering: A Feasibility Study

5a. CONTRACT NUMBER
W911NF-10-1-0397

5b. GRANT NUMBER

5c. PROGRAM ELEMENT NUMBER
611102

6. AUTHORS
Krishna Rajan, Mark E. Eberhart

5d. PROJECT NUMBER

5e. TASK NUMBER

5f. WORK UNIT NUMBER

7. PERFORMING ORGANIZATION NAMES AND ADDRESSES
Iowa State University of Science and Techn
Office of Sponsored Projects Administration
1138 Pearson Hall
Ames, IA 50011 -2207

8. PERFORMING ORGANIZATION REPORT NUMBER

9. SPONSORING/MONITORING AGENCY NAME(S) AND ADDRESS (ES)
U.S. Army Research Office
P.O. Box 12211
Research Triangle Park, NC 27709-2211

10. SPONSOR/MONITOR'S ACRONYM(S)
ARO

11. SPONSOR/MONITOR'S REPORT NUMBER(S)
56379-MS.25

12. DISTRIBUTION AVAILIBILITY STATEMENT
Approved for Public Release; Distribution Unlimited

13. SUPPLEMENTARY NOTES
The views, opinions and/or findings contained in this report are those of the author(s) and should not contrued as an official Department of the Army position, policy or decision, unless so designated by other documentation.

14. ABSTRACT
The objective of this program was to discover composition-charge density-property relationships. The motivation for this activity derived from density functional theory (DFT), which posits that all ground state molecular and solid-state properties are functionals of the charge density. Through this program we have demonstrated the feasibility of coupling advanced ab initio techniques with physical insight and informatics-based analysis to discover the nature of these relationships. The use of ab initio techniques were used to calculate the charge density of metals and alloys and reduce the density to physically meaningful parameters. This report describes the

15. SUBJECT TERMS
Charge density, Informatics, Statistical learning, Critical points, Density of states

16. SECURITY CLASSIFICATION OF:			17. LIMITATION OF ABSTRACT	15. NUMBER OF PAGES	19a. NAME OF RESPONSIBLE PERSON
a. REPORT	b. ABSTRACT	c. THIS PAGE			Krishna Rajan
UU	UU	UU	UU		19b. TELEPHONE NUMBER: 515-294-2670

Report Title

Charge Density Engineering: A Feasibility Study

ABSTRACT

The objective of this program was to discover composition-charge density-property relationships. The motivation for this activity derived from density functional theory (DFT), which posits that all ground state molecular and solid-state properties are functionals of the charge density. Through this program we have demonstrated the feasibility of coupling advanced ab initio techniques with physical insight and informatics-based analysis to discover the nature of these relationships. The use of ab initio techniques were used to calculate the charge density of metals and alloys and reduce the density to physically meaningful parameters. This report describes the accomplishments in linking ab initio data with informatics, first in terms of charge density and secondly in the related density of states (DOS). By uncovering relationships between the structure of the charge density and the elastic response, we have developed chemistry-charge density-property relationships. Similarly, we have (i) identified the features of the DOS which govern ground state crystal structure and (ii) "soft modeled" DOS for new alloy systems without requiring additional DFT calculations. We have shown that the charge density descriptors, when analyzed within a statistical framework, uncover previously unknown relationships between crystallographic structure and charge density.

Enter List of papers submitted or published that acknowledge ARO support from the start of the project to the date of this printing. List the papers, including journal references, in the following categories:

(a) Papers published in peer-reviewed journals (N/A for none)

Received		Paper
08/29/2011	1.00	Mark E. Eberhart, Scott Imlay, Craig Mackey, Travis E. Jones. Bond Bundles and the Origins of Functionality, The Journal of Physical Chemistry A, (08 2011): 0. doi: 10.1021/jp203013r
08/29/2011	2.00	Travis Jones, Mark Eberhart, Dennis Clougherty. Topological Catastrophe and Isostructural Phase Transition in Calcium, Physical Review Letters, (12 2010): 0. doi: 10.1103/PhysRevLett.105.265702
08/30/2011	3.00	Scott R. Broderick, Hafid Aourag, Krishna Rajan. Classification of Oxide Compounds through Data-Mining Density of States Spectra, Journal of the American Ceramic Society, (04 2011): 0. doi: 10.1111/j.1551-2916.2011.04476.x
08/30/2011	6.00	S. R. Broderick, K. Rajan. Eigenvalue decomposition of spectral features in density of states curves, Europhysics Letters, (09 2011): 57005. doi: 10.1209/0295-5075/95/57005
08/30/2011	5.00	Scott R. Broderick, Hafid Aourag, Krishna Rajan. Data mining of Ti–Al semi-empirical parameters for developing reduced order models, Physica B: Condensed Matter, (5 2011): 2055. doi: 10.1016/j.physb.2010.12.038
08/30/2011	4.00	P. V. Balachandran, S. R. Broderick, K. Rajan. Identifying the 'inorganic gene' for high-temperature piezoelectric perovskites through statistical learning, Proc. R. Soc. A, (03 2011): 2271. doi: 10.1098/rspa.2010.0543
08/30/2012	10.00	Chang Sun Kong, Wei Luo, Sergiu Arapan, Pierre Villars, Shuichi Iwata, Rajeev Ahuja, Krishna Rajan. Information-Theoretic Approach for the Discovery of Design Rules for Crystal Chemistry, Journal of Chemical Information and Modeling, (07 2012): 1812. doi: 10.1021/ci200628z
08/30/2012	12.00	Prasanna V. Balachandran, Krishna Rajan. Structure maps for A(4)(I)A(6)(II)(BO4)(6)X-2 apatite compounds via data mining, Acta Crystallographica Section B Structural Science, (01 2012): 24. doi: 10.1107/S0108768111054061
08/30/2012	11.00	Radislav Potyrailo, Krishna Rajan, Klaus Stoewe, Ichiro Takeuchi, Bret Chisholm, Hubert Lam. Combinatorial and High-Throughput Screening of Materials Libraries: Review of State of the Art, ACS Combinatorial Science, (11 2011): 579. doi: 10.1021/co200007w
08/30/2012	9.00	Krishna Rajan, Chang Sun Kong. Rational design of binary halide scintillators via data mining, Nuclear Instruments and Methods in Physics Research Section A: Accelerators, Spectrometers, Detectors and Associated Equipment, (07 2012): 145. doi: 10.1016/j.nima.2012.03.050
11/22/2013	22.00	Eric W. Bucholz, Chang Sun Kong, Kellon R. Marchman, W. Gregory Sawyer, Simon R. Phillpot, Susan B. Sinnott, Krishna Rajan. Data-Driven Model for Estimation of Friction Coefficient Via Informatics Methods, Tribology Letters, (05 2012): 0. doi: 10.1007/s11249-012-9975-y
11/22/2013	21.00	Subhas Ganguly, Chang Sun Kong, Scott R. Broderick, Krishna Rajan. Informatics-Based Uncertainty Quantification in the Design of Inorganic Scintillators, Materials and Manufacturing Processes, (07 2013): 0. doi: 10.1080/10426914.2012.736660

11/22/2013 23.00 Mark E. Eberhart, Travis E. Jones. Cauchy pressure and the generalized bonding model for nonmagnetic bcc transition metals,
Physical Review B, (10 2012): 0. doi: 10.1103/PhysRevB.86.134106

TOTAL: 13

Number of Papers published in peer-reviewed journals:

(b) Papers published in non-peer-reviewed journals (N/A for none)

Received	Paper
08/30/2012 13.00	Chang Sun Kong, Pierre Villars, Shuichi Iwata, Krishna Rajan. Mapping the 'materials gene' for binary intermetallic compounds—a visualization schema for crystallographic databases , Computational Science & Discovery, (07 2012): 15004. doi:
09/07/2012 15.00	Travis E. Jones, Mark E. Eberhart, Scott Imlay, Craig Mackey, Greg B. Olson. Better Alloys with Quantum Design, Physical Review Letters (accepted), (08 2012): 0. doi:
09/07/2012 16.00	Travis E. Jones, Mark E. Eberhart. The Two Faces of Chemistry: Can they be reconciled?, Foundations of Chemistry (Accepted), (08 2012): 0. doi:
09/07/2012 14.00	Mark E. Eberhart, Travis E. Jones. Cauchy Pressure and the Generalized Bonding Model, Physical Review B (accepted), (08 2012): 0. doi:
09/07/2012 17.00	Mark E. Eberhart, Scott Imlay, Craig Mackey, Travis E. Jones. Bond Bundles and the Origins of Functionality, Journal of Physical Chemistry A (In Press), (08 2012): 0. doi:
09/07/2012 18.00	Travis E. Jones, W. Li, X.F. Wang, Y.C. Zhou. Extreme Poisson's Ratios and their Electronic Origin in B2 CsCl-type AB Intermetallic Compounds, Physical Review B, (04 2012): 134108. doi:
09/07/2012 19.00	Travis E. Jones. The Role of Inter- and Intramolecular Bonding onImpact Sensitivity, Journal of Physical Chemistry A (Submitted), (08 2012): 0. doi:
09/07/2012 20.00	Travis E. Jones. Relativity and the Nobility of Gold, Nature (Submitted), (08 2012): 0. doi:

TOTAL: 8

Number of Papers published in non peer-reviewed journals:

(c) Presentations

Krishna Rajan, Iowa State University:

1. Discovering Materials Science through Data Science
Department of Materials Science and Engineering
Carnegie Mellon University
Pittsburgh PA. September 14th 2012

2. Informatics for Discovering the Materials Genome
Scientific Discovery Initiative Seminar Series
Pacific Northwest National Laboratory
Richland WA. September 19th 2012

3. Expanding the Design Limits in Materials via Data Mining
Symposium on Data Science Approaches for Mechanics of Materials
22nd International Workshop on Computational Mechanics of Materials
Baltimore Sept. 24-26th 2012

4. Informatics for the Inverse Design of Materials
49th Annual Society of Engineering Science Meeting
Atlanta GA; October 10-12, 2012

5. "omics" for Materials Science via Informatics
Symposium on Materials Informatics
Materials Research Society Fall 2012 meeting
Boston MA; Nov. 26th-30th 2012

6. Materials Co-Design for Translational Breakthroughs in Technology
Workshop on New and Novel Processes that are on the Verge of Industrial Modernization - Defense Materials Manufacturing and Infrastructure
National Academy of Sciences
Washington DC ; December 5th 2012,

7. Grand Challenges in Computational Materials Design Workshop
North Carolina State University
Raleigh, NC; Jan. 15-16th 201

8. Mapping the Materials Genome Landscape
1st International Conference on Molecular and Materials Informatics
Melbourne, Australia
February 4-6, 2013

9. Mapping the Electronic Structure Landscape for Materials Discovery
German Physical Society (DPG) meeting
Regenseberg, Germany
March 15th 2013

10. Enabling ICSME through Informatics and Big Data
Air Force Research Laboratory- Materials and Manufacturing Directorate
Wright Patterson Air Force Base
Dayton OH ; March 20th 2013

11. Informatics Aided Discovery of Energy Materials
2013 Kentucky Workshop on Renewable Energy and Energy Efficiency
Louisville KY ; March 25th 2013

12. Discovering Classfiers in Materials Science through Statistical Learning
Workshop on Machine Learning and Materials Science
Santa Fe Institute
Santa Fe , NM - April 3rd 2013

13. Nanoinformatics for Materials Chemistry
NSF Workshop - Cyberinfrastructure for Environmental Nanoinformatics
Center for Environmental Implications of Nanotechnology –UCLA

Los Angeles CA- May 7th 2013

14. Informatics for Ceramic Crystal Chemistry
Ceramics by Genome Symposium
10th Pacific Rim Conference on Ceramic and Glass Technology
San Diego, CA
June 6th 2013

15. Statistical Learning Guided Design of Materials
Fritz Haber Institute – Theory Group
Berlin , Germany
June 17th 2013

16. Developing Property Maps to Guide Materials Design via Statistical Learning
Summer Research Group Meeting – Materials by Design
Los Alamos National Laboratory
July 17, 2013

Number of Presentations: 16.00

Non Peer-Reviewed Conference Proceeding publications (other than abstracts):

Received Paper

TOTAL:

Number of Non Peer-Reviewed Conference Proceeding publications (other than abstracts):

Peer-Reviewed Conference Proceeding publications (other than abstracts):

Received Paper

TOTAL:

Number of Peer-Reviewed Conference Proceeding publications (other than abstracts):

(d) Manuscripts

Received		Paper
08/30/2011	8.00	Travis E. Jones, Mark E. Eberhart, Scott Imlay, Craig Mackey, Greg B. Olson. Quantum Design of an Iron Ceramic Interface, IN PREP (08 2011)
TOTAL:	**1**	

Number of Manuscripts:

Books

Received		Paper
11/22/2013	24.00	Krishna Rajan, editor. Informatics for Materials Science and Engineering, Waltham, MA: Butterworth-Heinemann, (08 2013)
TOTAL:	**1**	

Patents Submitted

Patents Awarded

Awards

Graduate Students

NAME	PERCENT_SUPPORTED	Discipline
Jonathan Miorelli	1.00	
Samantha Morgenstern	1.00	
John Graham	0.50	
FTE Equivalent:	**2.50**	
Total Number:	**3**	

Names of Post Doctorates

NAME	PERCENT_SUPPORTED
Claudia Loyola	1.00
FTE Equivalent:	**1.00**
Total Number:	**1**

Names of Faculty Supported

NAME	PERCENT_SUPPORTED	National Academy Member
Krishna Rajan	0.10	
Mark Eberhart	0.10	
FTE Equivalent:	**0.20**	
Total Number:	**2**	

Names of Under Graduate students supported

NAME	PERCENT_SUPPORTED	Discipline
Tim Wilson	1.00	Department of Chemical and Biological Engineering
FTE Equivalent:	**1.00**	
Total Number:	**1**	

Student Metrics

This section only applies to graduating undergraduates supported by this agreement in this reporting period

The number of undergraduates funded by this agreement who graduated during this period: 0.00

The number of undergraduates funded by this agreement who graduated during this period with a degree in science, mathematics, engineering, or technology fields:..... 0.00

The number of undergraduates funded by your agreement who graduated during this period and will continue to pursue a graduate or Ph.D. degree in science, mathematics, engineering, or technology fields:..... 0.00

Number of graduating undergraduates who achieved a 3.5 GPA to 4.0 (4.0 max scale):..... 0.00

Number of graduating undergraduates funded by a DoD funded Center of Excellence grant for Education, Research and Engineering:..... 0.00

The number of undergraduates funded by your agreement who graduated during this period and intend to work for the Department of Defense 0.00

The number of undergraduates funded by your agreement who graduated during this period and will receive scholarships or fellowships for further studies in science, mathematics, engineering or technology fields:..... 0.00

Names of Personnel receiving masters degrees

NAME
Total Number:

Names of personnel receiving PHDs

NAME
Total Number:

Names of other research staff

NAME	PERCENT_SUPPORTED
Scott Broderick	0.20
FTE Equivalent:	**0.20**
Total Number:	**1**

Sub Contractors (DD882)

1 a. Colorado School of Mines

1 b. Research Administration
1500 Illinois St
Golden CO 804011911

Sub Contractor Numbers (c):
Patent Clause Number (d-1):
Patent Date (d-2):
Work Description (e):
Sub Contract Award Date (f-1):
Sub Contract Est Completion Date(f-2):

1 a. Colorado School of Mines

1 b. Office of Research Services
1500 Illinois Street
Golden CO 804011911

Sub Contractor Numbers (c):
Patent Clause Number (d-1):
Patent Date (d-2):
Work Description (e):
Sub Contract Award Date (f-1):
Sub Contract Est Completion Date(f-2):

Inventions (DD882)

Scientific Progress

Technology Transfer

Charge Density Engineering: A Feasibility Study

Krishna Rajan: Department of Materials Science and Engineering, Iowa State University, Ames IA 50011

Mark E. Eberhart: Department of Chemistry & Geochemistry Colorado School of Mines Golden, CO 80401

ABSTRACT

The objective of this program was to discover composition-charge density-property relationships. The motivation for this activity derived from density functional theory (DFT), which posits that all ground state molecular and solid-state properties are functionals of the charge density. Through this program we have demonstrated the feasibility of coupling advanced *ab initio* techniques with physical insight and informatics-based analysis to discover the nature of these relationships. The use of *ab initio* techniques were used to calculate the charge density of metals and alloys and reduce the density to physically meaningful parameters. This report describes the accomplishments in linking *ab initio* data with informatics, first in terms of charge density and secondly in the related density of states (DOS). By uncovering relationships between the structure of the charge density and the elastic response, we have developed chemistry-charge density-property relationships. Similarly, we have (i) identified the features of the DOS which govern ground state crystal structure and (ii) "soft modeled" DOS for new alloy systems without requiring additional DFT calculations. We have shown that the charge density descriptors, when analyzed within a statistical framework, uncover previously unknown relationships between crystallographic structure and charge density.

BACKGROUND

As is known from density functional theory, the ground state properties of an atomic system are determined solely by its charge density. As mechanical response at typical strain rates is dominated by ground state properties, it may be possible to relate features of the charge density to specific mechanical properties. If these relationships could be combined with an understanding as to the effect of elemental composition on these electronic features, one could manipulate charge density so as to produce desirable properties. That is, one could design the chemistry of solids to yield optimum mechanical response. This program was designed to test these speculations. Specifically we explored two sets of relationships: first, a set that relates the geometry of the charge density to a material's elastic constants (a measure of a purely ground state mechanical property), and second, a set that relates elemental composition to the structure

of the charge density. Combined, these two sets provide the process-structure-property relationships for a new discipline of charge density engineering.

Our approach builds on the quantum theory of atoms in molecules (QTAIM), which has demonstrated that the structure of the charge density may be compactly represented by a few parameters describing the density around specific points. This "local approximation" reduces the description of a 3D scalar field—the charge density—to that of identifying the locations of the specified points and computing the values of shape descriptors at these points. This program used first principle calculations to create databases of charge density descriptors combined with physical/chemical arguments to identify meaningful combinations of these descriptors which are then subject to statistical and data mining techniques to establish correlations between these meaningful descriptors and measured or calculated single crystal elastic constants.

In previous work we have shown that the fcc single crystal elastic constant of simple metals can be correlated with the descriptors around a single critical point—the bond point. This correlation was demonstrated by inspection, with the introduction of a geometrically meaningful representation of the Hessian tensor in which the ρ_{11}, ρ_{22}, and ρ_{33} were combined to yield three new tensor invariants. In addition to this representation of the Hessian invariants at a critical point, there are many others, such as the Gaussian curvature, $G = \rho_{11}\rho_{22}\rho_{33}$, and the mean curvature or Laplacian, $L = \rho_{11}+\rho_{22}+\rho_{33}$. Attempts to extend this correlation between shape descriptors and elastic constants to other crystal structures were ultimately frustrated by the fact that the elastic constants were not dominated by the shape parameters around a single type of cp but around all cps. In these cases, we needed to look for correlations between elastic constants and often more than 20 shape parameters, which could be represented in several different meaningful forms.

We made significant progress in both the *ab initio* and informatics areas in the previous reporting periods, with the accomplishments of the two research thrusts fully integrated in the final year of the program, as discussed in this report. The previously reported accomplishments in *ab initio* included: (i) creation of a data set giving the shape parameters at all bcc and fcc transition metals at critical points; (ii) calculated the electronic structure of 160 B2 intermetallics and calculated their single crystal elastic moduli; (iii) located and calculated the shape parameters for ~80 of these compounds; (iv) constructed an empirical model to account for the observed trends in the single crystal B2 elastic constants; and (v) created a database of 30 entries to provide initial correlations of the effects of composition on shape descriptors. The previously reported progress in informatics analyses included: (i) performed a quantitative assessment of correlations between topological descriptors from critical points using data dimensionality reduction methods; (ii) confirmed that the chosen shape parameters may serve as robust modeling parameters for the next stage of the work by demonstrating that they serve as strong classifiers of crystal structure; and (iii) captured systematics in the impact of transition metal rare earth chemistry on B2 charge density shape descriptors.

The goals accomplishments in linking the informatics and *ab initio* aspects of this program which are the focus of this final report are summarized as follows. First, given the complexity of critical point data, the challenge is to link the shape of the charge density topology to chemistry and property, which represents a significant data challenge. To address this challenge, we have followed a two prong approach, where first we predict elastic moduli as a function of the charge density topology, which accomplishes: (i) accelerated prediction of elastic constant data, and (ii) reduced the amount of information needed from *ab initio* calculations. Given this limited knowledge requirement, we then predict the critical point descriptors based only on elemental descriptors from the periodic table. Therefore, the final outcome is that we can predict critical charge density values from basic elemental properties, and from these critical charge density values we can then predict the mechanical response, thus accelerating the selection of targeted chemistries. Additionally, we have studied the related DOS curves for both fundamental science and engineering purposes. The fundamental aspect of this approach is to answer the century old question of: why do metals have their ground state crystal structures? The engineering objective is to predict the DOS of alloys given the DOS of the constituent elements, and then from this informatics alloy DOS to extract the moduli. These integrated *ab initio* and informatics thrusts serve to guide future calculations, modify the chemical search space, and accelerate design of new materials for targeted electronic behavior.

Detailed Progress Report – Ab Initio **(Lead – Colorado School of Mines)**

(i) Building *ab-initio* database

In addition to several small data sets for the pure fcc and bcc transition metals, we completed the construction of a large data base of shape descriptors and elastic moduli for intermetallics with the B2 (CsCl) crystal structure. We chose to investigate 14 common B2 intermetallics and 128 RM (R = rare earth elements, M = metallic elements from groups 2, 8-13). These compounds were chosen to give a broad range of elastic responses. All calculations were performed with VASP using the PBE and PW91 generalized gradient approximations. We proceeded by generating the charge density on a 25 point/angstrom mesh, locating the CPs of the charge density, and generating the geometric properties of the charge density at those points, using our software package TECD. Notably, we discovered that there are two characteristic B2 topologies, one with second neighbor B-B bonds only, and one with both second neighbor A-A bonds and second neighbor B-B bonds (Figure 1). In both cases there are first neighbor A-B bonds. The single type of second neighbor bond topology is more common in this set of compounds. Only the 13 materials listed in Table 1 display both A-A and B-B bonds.

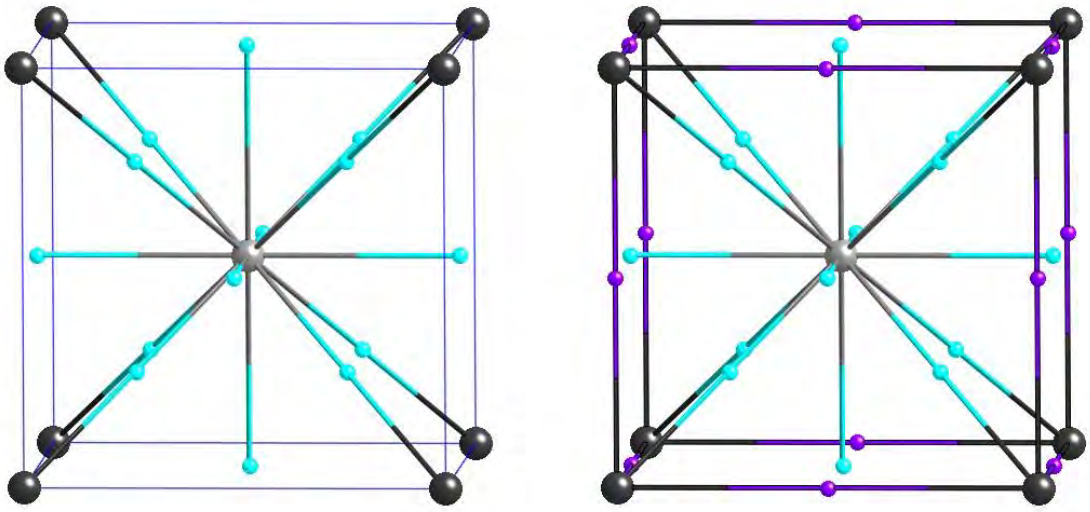

Fig 1: The two bonding topologies of the B2 compounds investigated. The A-B and B-B bonding topology is shown left, with turquoise spheres representing both first and second neighbor bond points. The A-B, A-A, and, B-B bonding topology is shown right, where the additional B-B bond points are shown as blue spheres.

Table 1: The B2s displaying both A-A and B-B second neighbor bonding.

AgHo	HgTb
AgNd	RhYb
AuCd	ZnEr
AuPr	ZnHo
CdLa	ZnTb
HgEr	ZnYb
HgNd	

In addition to calculating charge density we also calculated the elastic moduli of all the B2 crystals. The single crystal elastic moduli, C_{11}, C_{12}, and C_{44}, were computed from the curvature of the internal energy versus strain curves. The strains that resist C_{11}, C_{12}, and C_{44} are as follows:

(C_{11}) $\varepsilon_{11} = \varepsilon_{22} = \gamma$, $\varepsilon_{33} = (1+\gamma)^{-2}-1$
(C_{12}) $\varepsilon_{11} = \varepsilon_{22} = \varepsilon_{33} = \gamma$
(C_{44}) $\varepsilon_{12} = \varepsilon_{23} = \varepsilon_{31} = \gamma$

In all cases we calculated the internal energy using applied strains ranging from -0.025 to 0.025 in steps of 0.005. For the common B2 intermetallics, our calculated results agree with published experimental (calculated) results (Table 2). The independent shear constants are C_{44} and C' = $1/2(C_{11}-C_{12})$ and the strains resisted by these constants are depicted in Figure2.

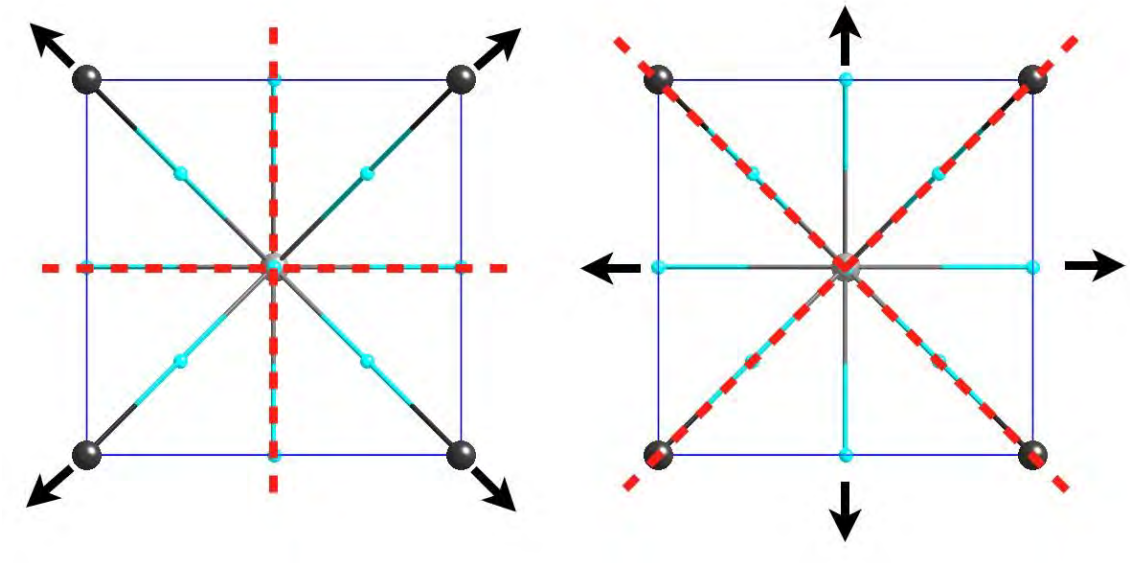

Fig 2: Strains with non-vanishing ε_{xy} (left) and $\varepsilon_{xx} = -\varepsilon_{yy}$ (right). The arrows represent the strain and the red dotted lines the nodes of that strain.

Table 2: A comparison of ab initio elastic properties of selected B2 intermetallics (this study) with the available reported data.

Phase	C_{11}(GPa)	C_{12}(GPa)	C_{44}(GPa)	A
CuZr	139.2	111.4	44.7	3.604
	137.3	108.9	44.9	3.160
	138.0	112.0	45.0	3.462
TiZn	140.7	107.2	97.0	5.791
	140.6	106.2	99.2	5.767
	143.5	99.0	94.0	4.225
NiTi	176.5	156.1	46.8	4.582
	179.5	156.4	49.5	4.291
	183.0	146.0	46.0	2.487
	178.2	147.6	49.0	3.202
AlZr	145.4	85.2 86.2	27.1	0.901
	145.7		29.8	1.000
CuZn	121.7	110.3	80.7	14.211
	123.4	110.9 116.0	84.3	13.480
	124.0		79.0	
AgMg	80.9	56.6	47.4	3.893
	79.8	55.5	47.8	3.930
AgZn	97.1	88.7	51.8	12.40
	97.3	88.0	54.0	11.54
AgCd	78.3	74.9	44.5	25.77
	76.8	72.7	45.1	22.27
AuZn	123.7	113.9	44.0	8.969
	124.1	113.5	46.8	8.830
AuCd	93.2	91.6	38.4	45.17
	91.8	89.9	39.6	42.75
AlTi	150.3	96.2	68.4	2.526
	150.9	97.6	70.1	2.630
NiAl	210.1	135.8 116.4	115.9	3.127
	207.0		106.8	3.172
PtTi	203.8	181.2	46.9	4.137
	203.3	182.2	48.5	4.592
PdTi	169.8	150.3	44.7	4.585
	168.6	150.4	45.9	5.049
CuY	115.0	47.6 47.1 47.4	35.8	1.062
	114.3	47.7	36.7	1.065
	116.4		34.5	1.000
	116.0		31.9	0.934
AgY	98.1	53.3 51.9 50.3	35.5	1.587
	96.1	54.5	35.7	1.615
	105.3		37.2	1.353
	102.4		32.6	1.361

Of the 142 B2 intermetallics for which the electronic structure was calculated, we were able to obtain reliable geometric charge density descriptors for 73 (Table 3). Our qualitative understanding is rooted in determining how the charge density responds to an applied strain, i.e. the nature of the charge flow or redistribution. Ideally, we would describe this charge flow using bond bundles [1, 2]. The B2 structure is characterized by only two types of bond bundles and as charge flows from one it must flow into the other, which makes the analysis of quantities that go as the ratio of bond bundle properties simpler to rationalize than those related to the absolute value of bb properties. One such property is the elastic anisotropy, $A = 2C_{44}/(C_{11}-C_{12})$. Hence, we began our development of a qualitative understanding of elastic response by attempting to correlate elastic anisotropy with critical point shape descriptors. Figure 3 shows the bond points of the common B2 structure. The crystal is composed of 8 first neighbor bond bundles, one connecting the central atom to each vertex, and 6 second neighbor bond wedges, one connecting the central atom to each face. By symmetry the nuclei of the bond bundles are pinned, along with the cage points. Ring points can, however, move in the (100) plane in the <110> direction, as shown in the lower panes of Fig. 3. Only movement of the ring point changes the volume of the bond bundles. We can then use the distance between the ring point and the first neighbor bond point as an indicator of the volume of the first neighbor bond bundle. Finally, we can get an approximation of the charge in the bond by multiply this distance by the number of electrons at the bond point.

Table 3: The chemical formula of the B2 intermetallics with reliable charge density descriptors.

AgDy	AuCd	CdDy	CdYb	HgHo	IrYb	RhTb
AgEr	AuDy	CdEr	CuDy	HgLa	PdDy	RhY
AgGd	AuEr	CdGd	CuEr	HgNd	PdEr	RhYb
AgHo	AuGd	CdHo	CuGd	HgPr	PdHo	ZnCe
AgLa	AuHo	CdLa	CuHo	HgSm	PdYb	ZnDy
AgNd	AuNd	CdNd	CuTb	HgTb	RhDy	ZnEr
AgPr	AuPr	CdPr	CuY	HgY	RhEr	ZnGd
AgSm	AuSm	CdSm	HgDy	IrEr	RhGd	ZnHo
AgTb	AuTb	CdTb	HgEr	IrHo	RhHo	ZnLa
AgY	AuY	CdY	HgGd	IrY	RhSm	ZnSm
ZnTb	ZnY	ZnYb				

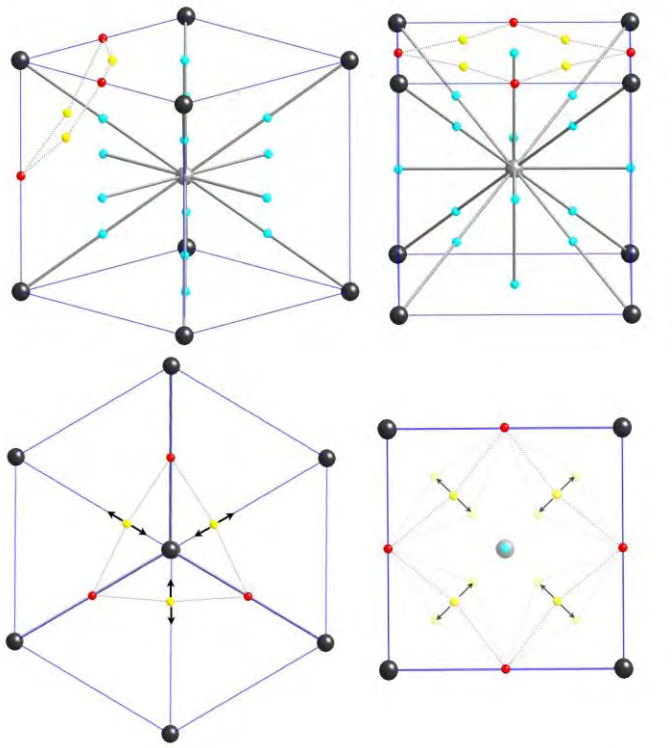

Fig 3: The edges of a first neighbor (left) and second neighbor bond bundle (right) in a B2 material. Bond points are shown as turquoise, rings as red, and cages as yellow spheres, while bond paths are shown as gray cylinders in the top to panes. The unit cell is composed of 8 1st neighbor bond bundles and 6 second neighbor bond wedges (half a bond bundle). The lower two panes show the cross section of the bond bundles with arrows indicating the directions the ring points can move. The semitransparent ring points also illustrate these directions.

We would expect that as this rough measure of charge increases the elastic anisotropy decreases because as the amount of charge in the first neighbor bonds increases so does the charge flow from/to those bonds. Fig. 4 supports this assumption. It is a plot of the distance between the ring and first neighbor bond point (in fractional coordinates) multiplied by the charge at the bond point versus the elastic anisotropy. From the above correlation we conclude that the Guassian curvature at the second neighbor bond points (cage points) correlates with C', but when we attempt to correlate C_{44} with eignevalues of H(cp) (or invariants of H(cp)), we find no good correlations. This observation is probably due to the fact that the charge flow to/from the CPs under strains with non-vanishing $\varepsilon_{xx} = -\varepsilon_{yy}$ occurs along the principal directions, whereas under a strain with non-vanishing ε_{xy} the charge flow is not along a principal direction. Such a phenomenon has, to our knowledge, not been reported. The simplest possible measure of this flow would be given by the curvature along the ring-bond ridge, as it is the direction of charge flow.

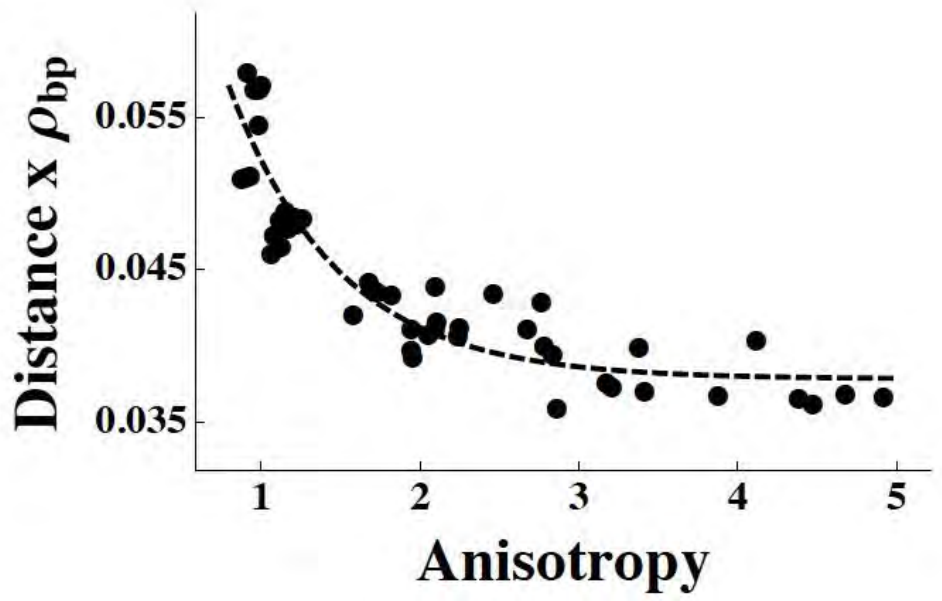

Fig 4: Plot of normalized distance (distance/lattice constant) between the ring point and 1st neighbor bond point multiplied by the charge density at the 1st neighbor bond point versus the calculated elastic anisotropy (2 $C_{44}/(C_{11}-C_{12})$. The normalized distance serves as an approximation of the volume of the 1st neighbor bond bundle.

(ii) *Generalized Bonding Model*

Just as a two-dimensional surface may be triangulated, a three dimensional volume, such as the charge density, may be covered by a set of irregular tetrahedra sharing faces edges and vertices. The resulting system is called a simplical complex. Being tetrahedral, the irreducible bundle forms a simplical complex over the charge density. In this unique form, the 1-skeleton or underlying graph of the simplical complex takes on special meaning. The 1-skeleton of a 3D simplical complex is the union of all the tetrahedral edges, which in this case is the set of all the system's 1-ridges and by default includes the bond-path, which is a 1-ridge connecting adjacent charge density maxima through a (3, -1) saddle point. Thus, the underlying graph contains as a subset the molecular graph common to depictions of the bonding in molecules and solids. Our conjecture is that the entire underlying graph (1-skeleton), as a set of pairwise connections between charge density critical points, provides an excellent quantitative representation of the bonding and elastic properties in a molecule or solid.

As a step in confirming this conjecture, we modeled inter-critical point spring constants by investigating crystalline systems. Our first effort was to recover the Cauchy pressure for the BCC transition metals, knowing only information about the charge density and its Hessian at the non-nuclear critical points. We started with the nonmagnetic BCC transition metals because, of the common crystal structures, only the BCC structure

possesses the simplest possible topology with one symmetry unique nuclear, bond, ring and cage CP and hence (the minimum) six different 1-ridges. We adopt the notation k_{cp1cp2} to denote the spring constant of the link joining cp1 to cp2, where a cp can be *n, b, r,* or *c* for nuclear, bond, ring and cage respectively. Thus, k_{br} corresponds to the spring constant of the bond to ring CP connection.

As with all cubic crystals, the elastic response of this entire set of springs is tied to three independent elastic constants: C_{11}, C_{12}, and C_{44} giving:

$$C_{11} = V_a^{-1/3} (0.67\, k_{nb} + 6.80\, k_{nr} + 2\, k_{nc} + 13.96\, k_{br} + 7.31\, k_{bc} + 14.56\, k_{rc})$$
$$C_{12} = V_a^{-1/3} (0.67\, k_{nb} + 1.60\, k_{nr} + 0\, k_{nc} + 8.76\, k_{br} + 3.31\, k_{bc} + 1.69\, k_{rc})$$
$$C_{44} = V_a^{-1/3} (0.67\, k_{nb} + 1.60\, k_{nr} + 0\, k_{nc} + 5.67\, k_{br} + 1\, k_{bc} + 0.80\, k_{rc})$$

where V_a is the atomic volume. Note that the quantity $C_{12} - C_{44}$, (the Cauchy pressure), is a function of only three spring constants

$$C_{12} - C_{44} = V_a^{-1/3} (3.10\, k_{br} + 2.31\, k_{bc} + 0.89\, k_{rc}),$$

where all terms related to connections with the nuclear cp have dropped out.

Systems where the Cauchy pressure is zero are indicative of, “atoms interacting through a central force potential,” which includes simple spring like connections and accounts for the fact that connections with the nuclear cp have dropped out. Positive deviations reflect “metallic bonding,” which necessitates corrections involving “many body interactions that result when an atom interacts with the electron gas of its neighbors.” Negative Cauchy pressures derive from “covalent bonding character” and require angular corrections. Our task reduced to finding relationships between the shape of the charge density at the connected critical points and the intercritical point spring constants.mGeometric and physical intuition suggested that the parameters of interest would be given the charge density at a critical point, ρ, and an angle, θ, related to the eccentricity of the charge density about the critical point, giving four descriptors for each intercritical point spring constant.

(iii) Energetic Materials

A picture of impact sensitivity based on the bond bundles of the electron charge density has been developed, which includes the response of both inter- and intramolecular bonding interactions. Impact sensitive materials were found to have closed intramolecular bond bundles with a low electron count that serves as a trigger linkage, while insensitive

materials do not. The shape and electron count of the intramolecular bond bundles was found to change between the gas phase and solid state due to the formation of intermolecular bonds. In the case of polynitrobenzenes this change was subtle and did not affect the trigger linkages. However, the intermolecular bonds in crystalline RDX transform the C-N trigger linkages found in the gas phase to N-N trigger linkages in the solid state. This observation offers a theoretical justification of the well-known experimentally observed differences in the decomposition of gas phase and crystalline RDX.

(iv) Critical Point Input into Informatics Analysis

Table 4. A list of descriptors for electronic charge density topology of intermetallic materials. These values were calculated for the B2 intermetallics listed in Table 3. These descriptors were analyzed by informatics for developing structure-property relationships, where the property is based on the elastic moduli.

No.	Descriptor	Description
1	λ_{1_bb}	Eigenvalue 1 at the bond-bundle critical points
2	λ_{2_bb}	Eigenvalue 2 at the bond-bundle critical points
3	λ_{3_bb}	Eigenvalue 3 at the bond-bundle critical points
4	ρ_{bb}	Charge at the bond-bundle critical points
5	$\tan(\theta)_{bb}$	$(\lambda_{2\_bb} / \lambda_{1\_bb})^{1/2}$
6	$\Delta_{\_bb}$	Laplacian $(=\lambda_{1\_bb} + \lambda_{2\_bb} + \lambda_{3\_bb})$
7	λ_{1_b}	Eigenvalue 1 at the bond critical points
8	λ_{2_b}	Eigenvalue 2 at the bond critical points
9	λ_{3_b}	Eigenvalue 3 at the bond critical points
10	ρ_b	Charge at the bond critical points
11	$\tan(\theta)_b$	$(\lambda_{2\_b} / \lambda_{1\_b})^{1/2}$
12	$\Delta_{\_b}$	Laplacian $(=\lambda_{1\_b} + \lambda_{2\_b} + \lambda_{3\_b})$
13	λ_{1_c}	Eigenvalue 1 at the cage critical points
14	λ_{2_c}	Eigenvalue 2 at the cage critical points
15	λ_{3_c}	Eigenvalue 3 at the cage critical points
16	ρ_c	Charge at the cage critical points
17	$\Delta_{\_c}$	Laplacian $(=\lambda_{1\_c} + \lambda_{2\_c} + \lambda_{3\_c})$
18	λ_{1_r}	Eigenvalue 1 at the ring critical points
19	λ_{2_r}	Eigenvalue 2 at the ring critical points
20	λ_{3_r}	Eigenvalue 3 at the ring critical points
21	ρ_r	Charge at the ring critical points
22	$\Delta_{\_r}$	Laplacian $(=\lambda_{1\_r} + \lambda_{2\_r} + \lambda_{3\_r})$
23	f_1	Electron density flatness $(=\rho_c^{min}/\rho_b^{max})$
24	f_2	Energy term related to stacking fault $(=(\rho_b - \rho_c)^2)$
25	f_3	Energy term related to surface $(=(\rho_b + \rho_c)^2)$

Detailed Progress Report – Informatics **(Lead – Iowa State University)**

(i) Genetic Programming for QSPRs

Genetic programming is an approach that has been applied for optimizations in many engineering fields such as process control. We apply it for the first time to *ab initio* derived data to predict the elastic constants of transition metals as a function of critical point shape descriptors. This work serves two purposes: (i) QSPR can be used to screen for material properties and accelerate the identification of new candidate materials; and (ii) the terms in the QSPR model provide physical understanding of material behavior that otherwise is too complex to identify.

We have used genetic programming [2] to obtain a function of the charge density shape descriptors which gives the spring constants of the intercritical point connections. GP is an evolutionary algorithm based on the ideas of biological evolution, designed to evolve computer programs that optimize a user-defined function. The objective is to create a population of possible solutions to the problem. The members of the population are evaluated using a fitness function (in this case the mean of the squared prediction errors for each of the five BCC metals) that measures how good the functions are in predicting the desired quantity (Cauchy pressure) from the (shape) descriptors.

A genetic programming search was conducted for a function that would express the spring constant between two critical points as a function of four variables mentioned above. Certain constraints were imposed on the function, such as maintaining symmetry and simplicity of the model to make physical interpretation possible. The fitness function was set to the mean of the squared deviations of the predicted value of Cauchy pressure from the value calculated through DFT. Two different function forms were found that obeyed the defined criteria and were highly accurate:

Function 1:

$$k_{cp1cp2} = \frac{0.1079(\frac{2\pi}{3} - \theta_{cp1})(\frac{2\pi}{3} - \theta_{cp2})}{\rho_{cp1}\rho_{cp2}}$$

.

Function 2:

$$k_{cp1cp2} = 18.22(0.5784 - \rho_{cp1})(0.5784 - \rho_{cp2})(2.063 - \theta_{cp1})(2.063 - \theta_{cp2})$$

Function 1 is optimized for simplicity and predicts the Cauchy pressure with more than 97% accuracy. A slightly better accuracy of prediction (98.6%) is possible with Function

2, though at the cost of the simplicity of the relation between the spring constant and the critical point descriptors. The plots for the predicted and actual Cauchy pressure calculated through DFT are presented in Figure 5.

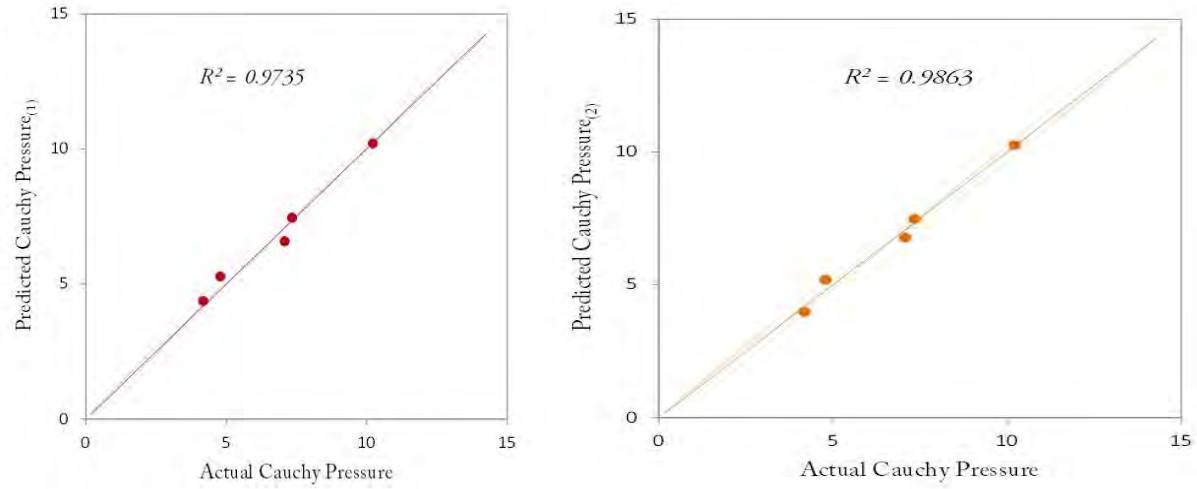

Figure 5. Genetic programming prediction of Cauchy pressure versus the DFT predicted Cauchy pressure for bcc transition metals. The model optimized for simplicity has 97.3% accuracy, while the model optimized for accuracy has 98.6% accuracy.

Our analysis of these two functional forms provides insight as to the origin of the intercritical point spring constant. The Cauchy pressure goes to zero when the charge density takes on a shape resulting from the overlap of spherically symmetric densities. This "reference state," though built from overlapping spherical charge densities, will likely be characterized by a BCC topology with nonzero values for all the shape descriptors of the observed systems.

If we assume the tails of these overlapping spherical charge densities go as $e^{-\alpha r}$. It is then an easy matter to calculate the values of the reference quantities as functions of α. While the reference quantities, ρ and θ, vary with α, k_{cp1cp2}, as calculated be either Function 1 or Function 2, vary more slowly and are close to zero**.** The compelling conclusion is that the inter-critical point spring constants provide information about the amount of charge that flows from a CP in its reference state to yield the same CP in the observed state; a number of functional forms may scale with the "distance" between these two states.

If we are to generalize this work to different topologies, we must identify a true invariant of overlapping spherical charge densities, or, a best method to estimate the values of the shape descriptors for the reference state of given element in a given crystal structure.

(ii) Design Rules for New Intermetallics

The predictions of mechanical property as a function of charge density has been extended to intermetallic compounds, with elastic constants predicted as a function of 25 shape descriptors. Additionally these descriptors are used to predict the stability of a compound; that is, to predict whether a new material could form in a particular crystal structure. These results have been tested on known systems, while future work will expand this work to suggest new candidate materials.

We found that the predictive models achieved by correlating topological charge density in terms of critical points with elastic constants discloses the hidden structure-property relationships that cannot be identified from crystallographic information. The results for prediction of the elastic constants from the charge density critical points are provided in Figure 6. Our results demonstrate that charge density topology data of a material system contains the information required for the prediction of elastic constants of a new material.

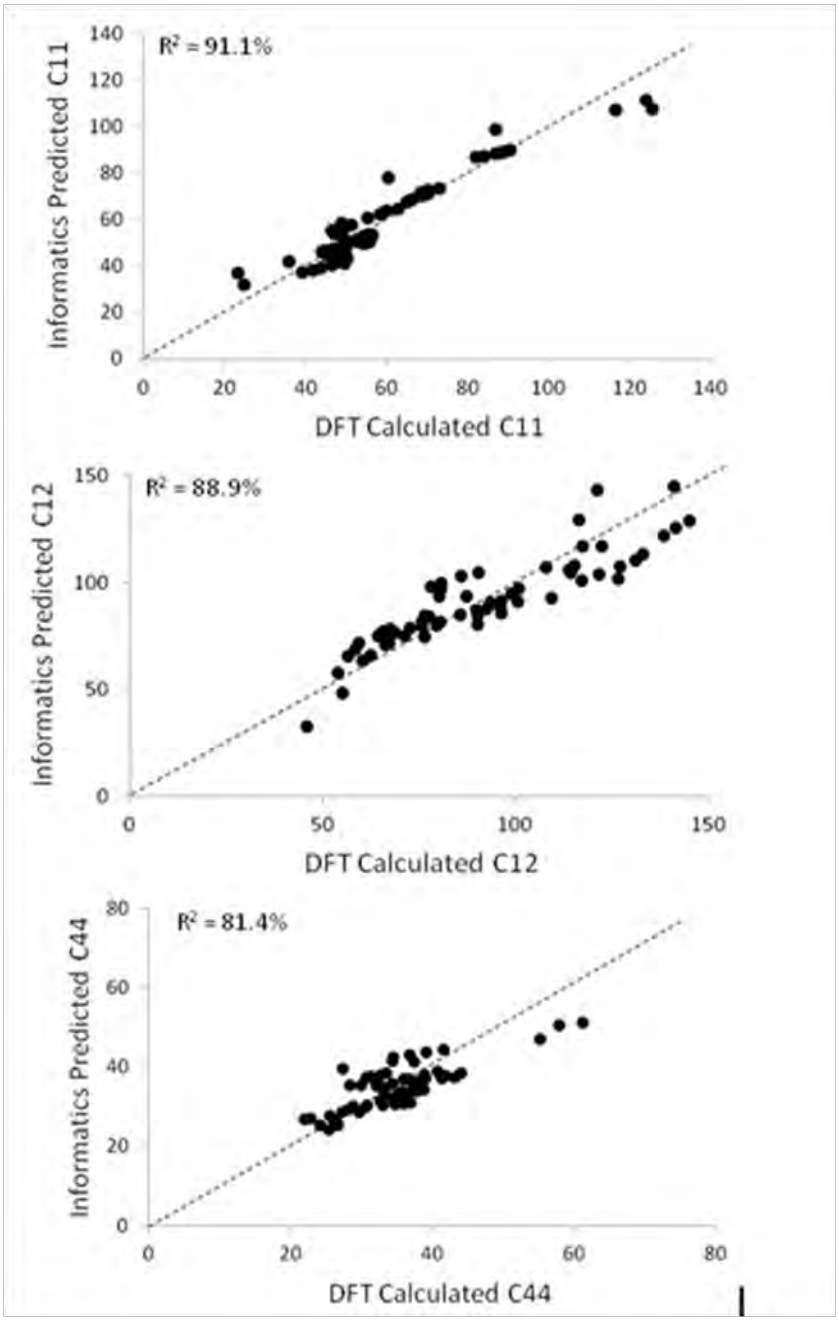

Figure 6. Prediction of elastic constants based on a partial least squares regression model of 73 intermetallic compounds. The accuracy of this approach demonstrates the ability to predict mechanical properties for alloys.

In addition to predicting mechanical properties, we have developed a series of design rules for predicting mechanical stability of new compounds, building on the ability to define mechanical properties as a function of critical point descriptors. For a cubic crystal, the following three conditions are generally accepted as the elastic stability criteria:

(i) Bulk modulus, $K = 1/3(C_{11} + 2C_{12}) > 0$

(ii) Shear modulus, $G = C_{44} > 0$

(iii) $C_{prime} = 1/2(C_{11} - C_{12}) > 0$

If all of these three conditions are not met simultaneously, the cubic crystal is (mechanically) unstable. The charge density data were correlated with the stability condition using a recursive partitioning algorithm. As a result, if-then rules of stability criteria were developed as shown in Figure 7. Only five critical point descriptors were selected for building the tree model, indicating that those five descriptors are the defining factors for the determination of stability condition for B2 compounds. Starting from the root node of the if-then tree structure, the stability of a new material can be predicted. According to the internal validation of the model, R^2=0.8526 was obtained. This shows that the elastic stability of a material can be predicted directly from the electronic charge density information of the material.

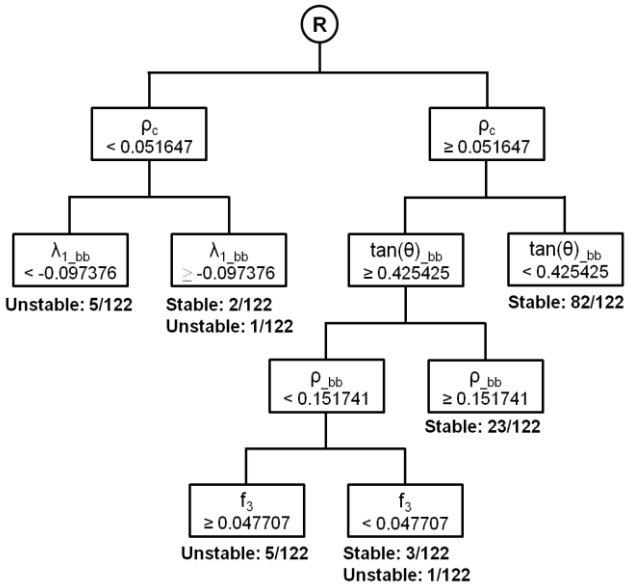

Figure 7.Classification tree model for the prediction of the stability of B2 compounds in terms of the critical points of topological charge density; the numbers shown at the end of each branch indicate the number of potential new compounds classified into each branch.

(iii) Identification of Minimal Electronic Structure Information

One of the primary objectives of informatics is to identify the minimal amount of information necessary for describing a material. To this end, we have applied principal component analysis (PCA) and variable importance parameter (VIP) in identifying the parameters which are most important in describing electronic structure. By identifying the fewest parameters needed to model the elastic moduli from the charge density topology, the informatics modeling of these parameters becomes manageable, as discussed in the next section.

To identify the aspects of the charge density topology which most impact the elastic constants, VIP was applied to the complete set of parameters describing the CPs for the intermetallic compounds. The results of Figure 8 show that all of the CP descriptors are not equally significant for the estimation of elastic constants. Additionally different CP descriptors affect the different constants, and therefore different topological features of electronic structure play the major role in determining the mechanical behaviors. The most significant descriptors, which are defined as those having 'Variable Importance' measures greater than unity, are then used with predictive informatics – partial least squares (PLS) - to develop the QSARs. For C_{11}, 17 variables meet the importance criteria, 21 variables for C_{12}, and 11 variables for C_{44}. Of these variables, charge at the cage critical points is very significant for C_{44}, shape at the ring critical points is very significant for C_{12}, and charge at the ring critical points and the energy term related to the surface have significance for all of the elastic constants, and therefore also anisotropy and Cauchy pressure. These findings for the B2 intermetallics are much different than the descriptor (charge around bond critical point) previously discussed as controlling the FCC mechanical behavior. While charge at bond critical point is significant for all three constants, it has relatively minor effect as compared to other descriptors. A heat map was created for the descriptor data base to further select the relevant descriptors based on further selection criteria (Figure 9). Based on this further selection criteria, all relevant descriptors were identified (Table 5). We identify based on the descriptors identified as determining elastic constants, C_{11} and C_{44} are determined by the charge density at the critical points, while C_{12} is determined by the shape at the critical points.

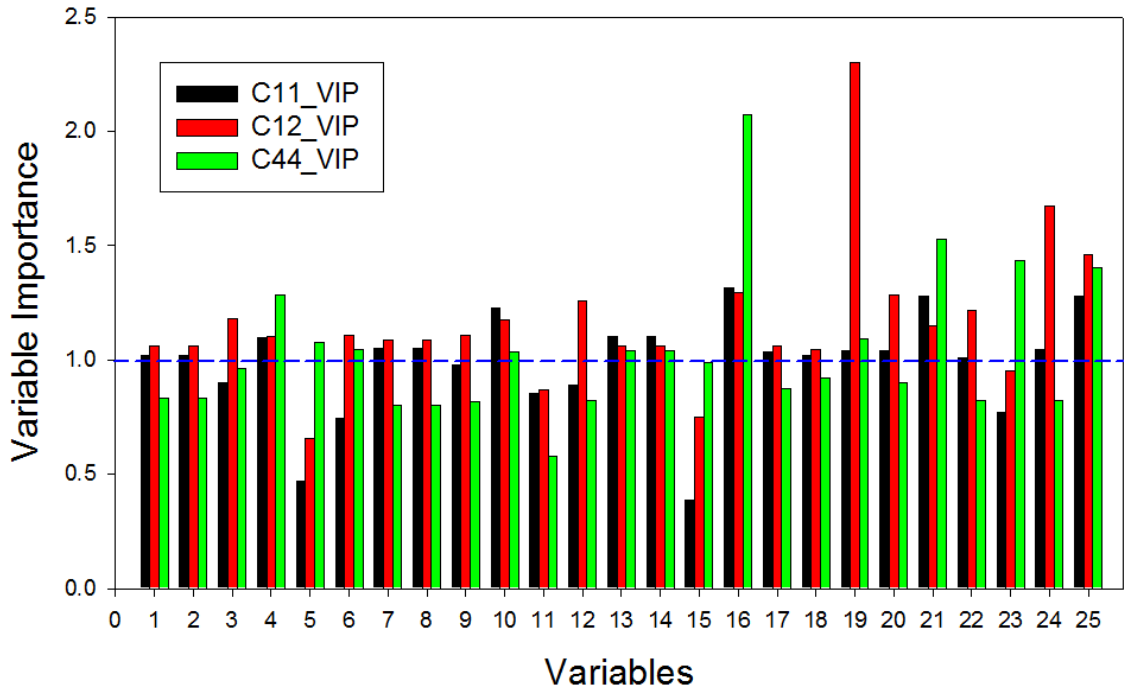

Figure 8. The importance measure of topological charge density descriptors with respect to the elastic constant of intermetallic compounds, which is obtained by variable importance in the projection (VIP) scores for the key predictor selection. The cut-off value of VIP is unity. 1. λ_{1_bb}*; 2.* λ_{2_bb}*; 3.* λ_{3_bb}*; 4.* ρ_{bb}*; 5.* $\tan(\theta)_{bb}$ $(=(\lambda_{2\_bb} / \lambda_{1\_bb})^{1/2})$*; 6.* $\Delta_{\_bb}$ $(=\lambda_{1\_bb} + \lambda_{2\_bb} + \lambda_{3\_bb})$*; 7.* λ_{1_b}*; 8.* λ_{2_b}*; 9.* λ_{3_b}*; 10.* ρ_b*; 11.* $\tan(\theta)_b$ $(=(\lambda_{2\_b} / \lambda_{1\_b})^{1/2})$*; 12.* $\Delta_{\_b}$ $(=\lambda_{1\_b} + \lambda_{2\_b} + \lambda_{3\_b})$*; 13.* λ_{1_c}*; 14.* λ_{2_c}*; 15.* λ_{3_c}*; 16.* ρ_c*; 17.* $\Delta_{\_c}$ $(=\lambda_{1\_c} + \lambda_{2\_c} + \lambda_{3\_c})$*; 18.* λ_{1_r}*; 19.* λ_{2_r}*; 20.* λ_{3_r}*; 21.* ρ_r*; 22.* $\Delta_{\_r}$ $(=\lambda_{1\_r} + \lambda_{2\_r} + \lambda_{3\_r})$*; 23.* f_1 $(=\rho_c^{min}/\rho_b^{max})$*; 24.* f_2 $(=(\rho_b - \rho_c)^2)$*; 25.* f_3 $(=(\rho_b + \rho_c)^2)$

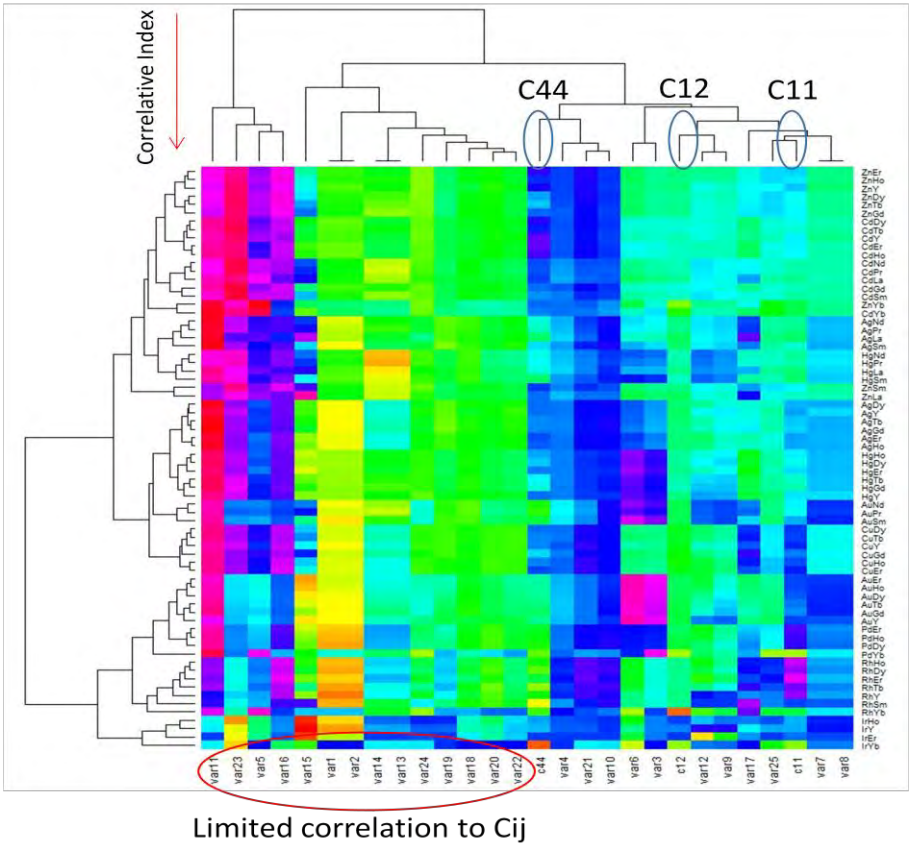

Figure 9. Heat map and dendrograms for the descriptor space of Table 1 and the corresponding elastic constants. This figure maps out the correlation between the descriptors and demonstrates the complexity of the input data base, thus demonstrating the necessity of data mining. From this map, we identify additional descriptors that were not identified through VIP. The additional descriptor potentially relevant for modeling the elastic constants are shown in Table 2.

Table 5. A list of descriptors identified as most significant for the respective elastic constants using VIP and heat map. The descriptors defined as most important are based on their selection by both methods. When considered in magnitude of importance, we find that the charge at the bond critical point (ρ_b), the shape at the ring critical point (λ_{2_r}), and the charge at the cage critical point (ρ_c) dictate C_{11}, C_{12}, and C_{44}, respectively.

	C11	**C12**	**C44**
VIP	p_b, p_c, p_r, f_3	λ_{2r}, f_2, f_3	p_c, p_r, f_1, f_3
Heat map	f_3	Δ_r, λ_{3b}	p_{bb}, p_r, p_b
Selected	**p_b, p_c, p_r, f_3**	**f_2, f_3, λ_{2r}, λ_{3b}, Δ_r**	**p_b, p_c, p_r, p_{bb}, f_1, f_3**

(iv) Informatics Modeling of Critical Point Descriptors

From the developed quantitative structure-property relationship (QSPR), the charge at the bond critical points (ρ_b), the shape at the ring critical points (λ_r), and the charge at the cage critical points (ρ_c) were identified as the most important features for determining C11, C12, and C44, respectively (Table 5 and Figure 10). While that work accelerated the selection of chemistries for targeted elastic behavior, it still required the DFT calculation of the critical point descriptors. To address this limitation, we use an informatics based approach to "learn" the mathematics of the DFT calculation and predict these critical point values for thousands of chemistries in seconds. Thus this work developed the use of informatics for approximating the complex mathematics of DFT, and is used for targeted charge density and elastic behavior design. The input into the analysis is shown in Table 6, with the results of the descriptor inputs shown in Figure 11. From this analysis, we identified the minimum number of elemental descriptors required to describe the charge density topology and the mechanical response.

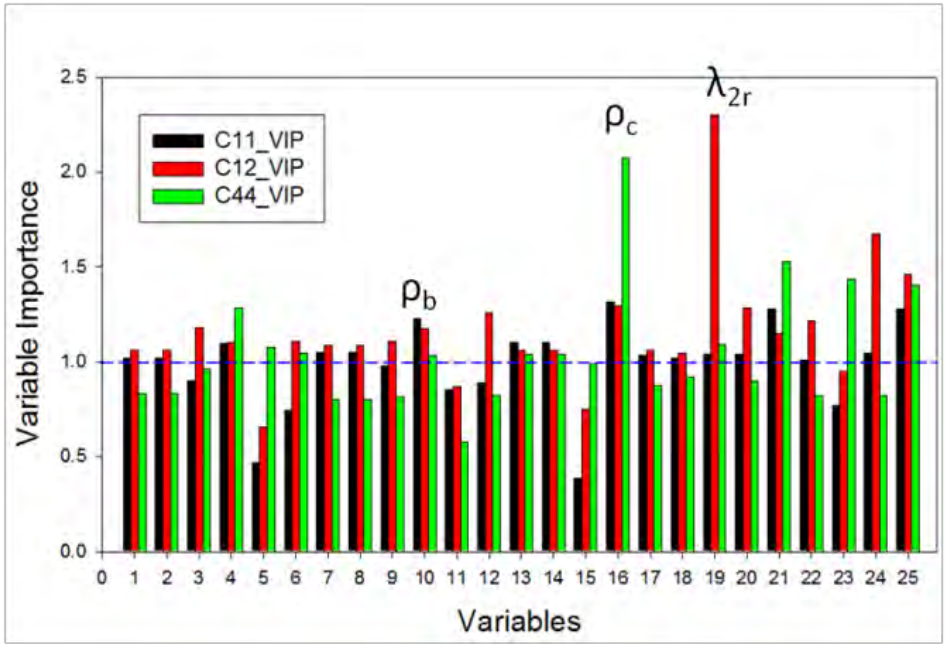

Figure 10. The elastic constants (C11, C12, and C44) were modeled as a function of charge density critical points. Using a variable importance in the projection approach to identify the most critical charge density descriptors for each elastic constant, and then a partial least squares analysis of these descriptors, the controlling charge density features were identified. For C11 charge at the bond critical point was most important, for C12 shape at the ring critical point was most important, and for C44 charge at the cage critical point was most important. We now predict these three critical points as a function of the elemental components of the intermetallics.

Table 6. Input into the PLS analysis. The first three columns are the DFT calculated critical point descriptors.

				Element A					Element B				
TMRE	charge_b	eig2_r	charge_c	Pseudopotential core radii sum $R=r_c+r_s$	Pauling electronegativity	Melting Point (K)	Atomic Weight	Density @ 293 K (g/cm³)	Pseudopotential core radii sum $R=r_c+r_s$	Pauling electronegativity	Melting Point (K)	Atomic Weight	Density @ 293 K (g/cm³)
AgCa	0.09953	0.146708	0.05047	2.375	1.93	1235.08	107.8682	10.5	3	1	1112	40.078	1.55
AgI	0.12461	0.157876	0.042866	2.375	1.93	1235.08	107.8682	10.5	1.585	2.66	386.7	126.90447	4.93
AgMo	0.262139	0.218766	0.165314	2.375	1.93	1235.08	107.8682	10.5	2.72	2.16	2890	95.94	10.22
AgSc	0.167966	0.29196	0.090283	2.375	1.93	1235.08	107.8682	10.5	2.75	1.36	1814	44.95591	2.989
AgTi	0.178147	0.187461	0.131953	2.375	1.93	1235.08	107.8682	10.5	2.58	1.54	1933	47.88	4.54
AgW	0.290246	0.272657	0.173413	2.375	1.93	1235.08	107.8682	10.5	2.735	2.36	3680	183.84	19.3
AgY	0.151633	0.208017	0.076263	2.375	1.93	1235.08	107.8682	10.5	2.94	1.22	1795	88.90585	4.469
KRe	0.119693	0.178391	0.048341	3.69	0.82	336.8	39.0983	0.862	2.68	1.9	3453	186.207	21.02
KW	0.108844	0.124221	0.051475	3.69	0.82	336.8	39.0983	0.862	2.735	2.36	3680	183.84	19.3
MnMg	0.201297	0.074334	0.034449	2.22	1.55	1517	54.93805	7.44	2.03	1.31	922	24.305	1.738
MnSc	0.213869	0.191127	0.139318	2.22	1.55	1517	54.93805	7.44	2.75	1.36	1814	44.95591	2.989
MnW	0.370212	0.025284	0.252933	2.22	1.55	1517	54.93805	7.44	2.735	2.36	3680	183.84	19.3
MnY	0.191783	0.21734	0.114336	2.22	1.55	1517	54.93805	7.44	2.94	1.22	1795	88.90585	4.469
MoSc	0.203182	0.193447	0.141205	2.72	2.16	2890	95.94	10.22	2.75	1.36	1814	44.95591	2.989
MoSr	0.136147	0.150869	0.073498	2.72	2.16	2890	95.94	10.22	3.21	0.95	1042	87.62	2.54
MoY	0.191951	0.17474	0.11486	2.72	2.16	2890	95.94	10.22	2.94	1.22	1795	88.90585	4.469
NbOs	0.363461	0.094869	0.213102	2.76	1.6	2741	92.90638	8.57	2.65	2.2	3327	190.23	22.59
NbRe	0.360153	0.012579	0.215449	2.76	1.6	2741	92.90638	8.57	2.68	1.9	3453	186.207	21.02
NbY	0.170374	0.123822	0.114401	2.76	1.6	2741	92.90638	8.57	2.94	1.22	1795	88.90585	4.469
NiSc	0.205029	0.288946	0.116457	2.18	1.91	1726	58.6934	8.902	2.75	1.36	1814	44.95591	2.989
NiY	0.181377	0.271383	0.096722	2.18	1.91	1726	58.6934	8.902	2.94	1.22	1795	88.90585	4.469
PdSc	0.199427	0.364942	0.101276	2.45	2.2	1825	106.42	12.02	2.75	1.36	1814	44.95591	2.989
PdY	0.180207	0.328806	0.083401	2.45	2.2	1825	106.42	12.02	2.94	1.22	1795	88.90585	4.469
PtSr	0.142257	0.334298	0.048756	2.7	2.28	2045	195.08	21.45	3.21	0.95	1042	87.62	2.54
PtY	0.20336	0.419897	0.083722	2.7	2.28	2045	195.08	21.45	2.94	1.22	1795	88.90585	4.469

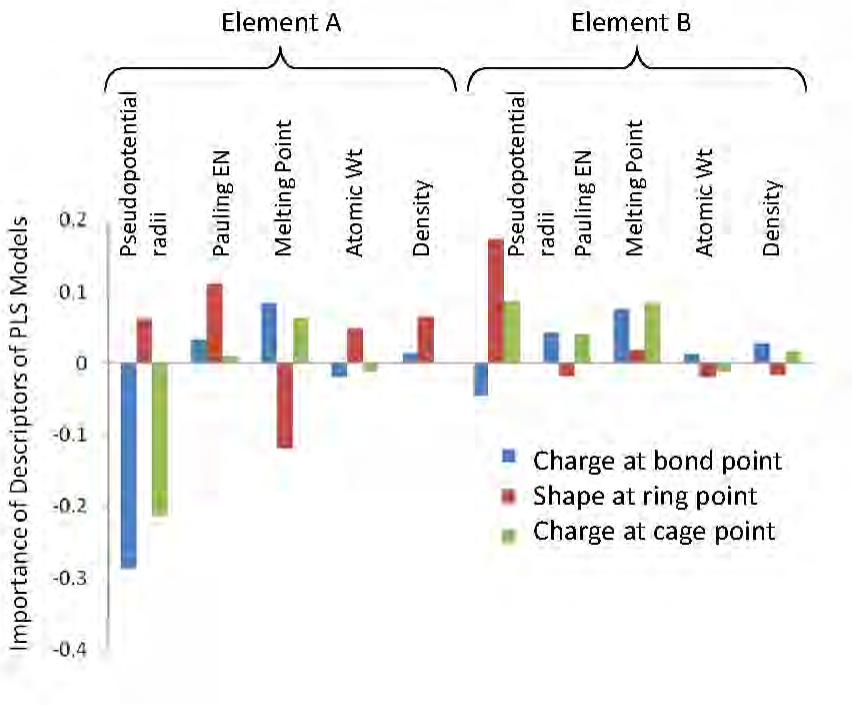

Figure 11. Weights of the PLS model, standardized based on different units of inputs. As can be seen, the shape descriptor is much different than the charge descriptors (opposite sign for multiple descriptors), while the two charge descriptors are similar, particularly for the transition metal. To accelerating the modeling of the charge density topology, we predict those descriptors with high magnitude weight, and remove those descriptors with low weight.

Using this reduced descriptor space from VIP analysis of the high-dimensionality charge density description, we applied partial least squares (PLS), a predictive informatics approach which accounts for multi-collinearity in high dimensional data, we predicted the charge density critical points, which we showed in Figure 6 can then be used to model the elastic moduli. The results of this prediction is shown in Figure 12.

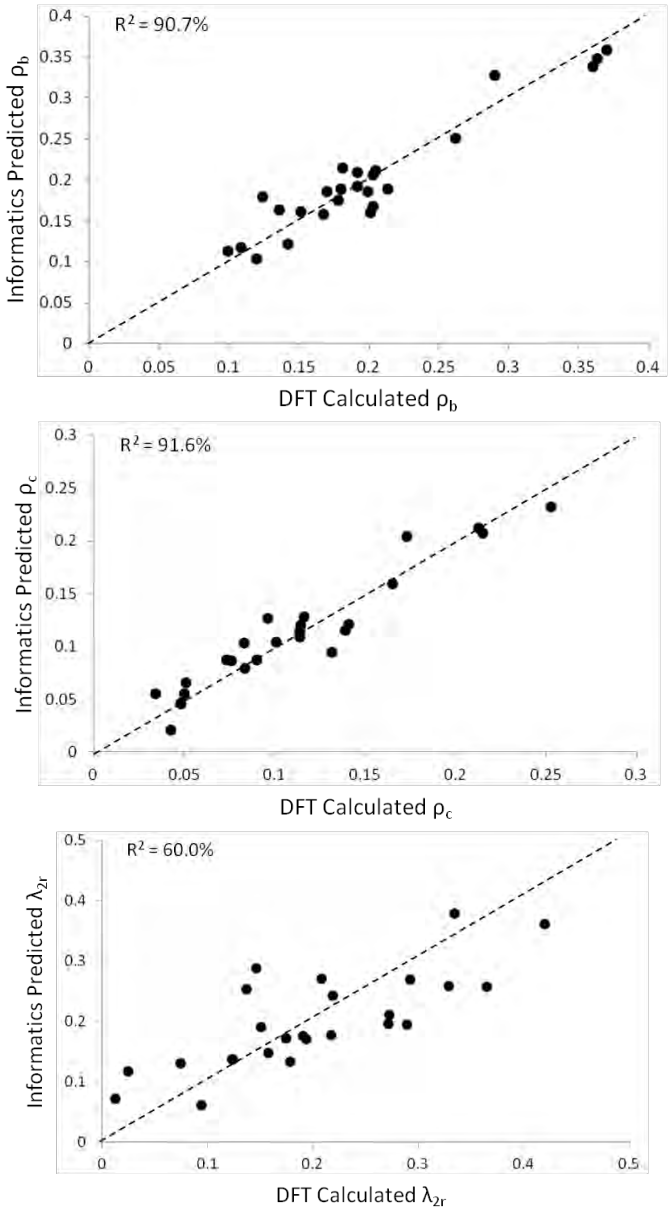

Figure 12. Result of the PLS analysis. Based on the input descriptors, the charge at the bond and cage critical points were modeled with high accuracy, demonstrating that informatics was able to accurately model these aspects of the charge density without requiring any additional DFT calculations. However, the accuracy for the shape descriptor was insufficiently accurate, implying that the controlling physics is different than it was for the charge.

In Figure 12, we found that the elemental descriptors of Figure 11 were sufficient for modeling the charge density at the critical points. However, for modeling the shape at the critical points, these descriptors were insufficient. Through further informatics analysis, we found that to model the shape at the critical points, the elemental work functions must be added. When the work function is included, the accuracy of the prediction of shape improves by over 50% (Figure 13).

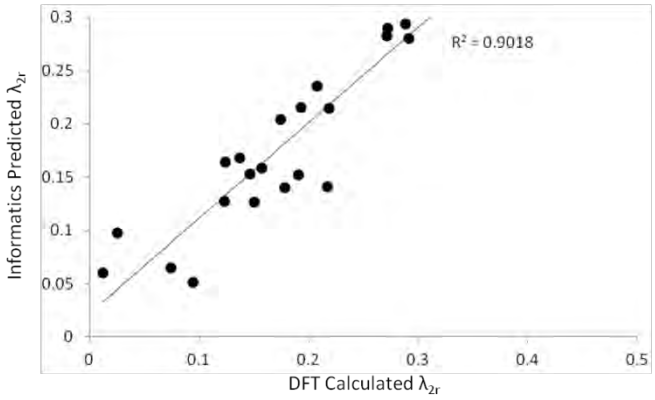

Figure 13. Improvement in prediction of λ_{2r} by adding work function into the predictor set. Accuracy improved from 60% to 90%. The difference between charge density at the critical points and shape of the charge density topology of the critical point is described by the work functions of the constituent elements.

We can thus predict the elastic moduli from the critical point descriptors and we can now model the critical point descriptors from descriptors of the elements comprising the alloy. Based on this, we can now predict the electronic structure and mechanical response of 'virtual' materials based only on information from the periodic table. This work significantly accelerates the targeted design of new materials based on electronic structure design.

(v)Accelerated Design Based on Density of States

From the DOS spectra, and particularly from the symmetry induced d-orbital splitting, of each transition metal in each of bcc, fcc, and hcp structure (provided by the CSM group), we have applied informatics methods to these d-orbital splittings to predict the ground state structure of the transition metals (Figure 14). The prediction based on pattern recognition and partial least squares regression is found to work very well for this class of material.

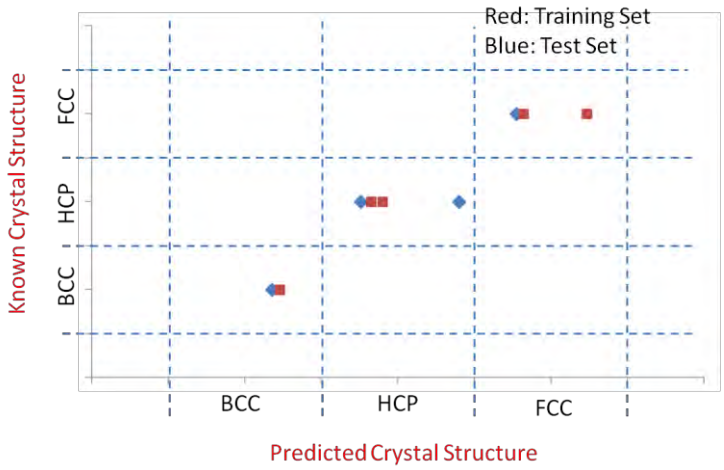

Figure 14.Informatics prediction of ground state crystal structure of second row transition metals. The model predicts crystal structure from a DOS input of each element in three structures: fcc, bcc, and hcp structures. The red squares are elements used in training the model, while the blue diamonds are elements which were not included in building the model but were used instead for external validation.

Building on this structural modeling from DOS curves, we use the approach to model unknown DOS spectra using artificial neural networks (ANN). Using an input of DOS of Fe, Ni, Pd, Fe_3Ni, $FeNi_3$, Fe_3Pd, and $FePd_3$, a model linking these elemental DOS to multi-component alloys was developed. This model is then tested using other known alloy DOS not used in model development. The necessary input to model these systems are the DOS spectra for Fe (FCC), Pd (BCC) and Ni (BCC). Also DOS spectra of two alloys in each system were introduced so that the learning technique can capture the nature of the interactions of elements within alloys. Along with the DOS spectra of the elements of the binary systems, the DOS spectra of two chemistries of each binary system were used to train the model. The model was tested for FePd and FeNi (Figure 15), which were not included in any form in training of the model, but were used solely for testing the accuracy of the model. Figure 15 shows these DOS spectra with the prediction compared to DFT. The model for predicting DOS of alloy systems shows a level of accuracy, with the general shape of the DOS curve captured but the fine structure is not fully captured. The model therefore links the elemental DOS with the alloy DOS. Of particular note is that crystal structure is not explicitly defined in this analysis. The only description of the alloy necessary is the stoichiometry. For the results shown, the input for Fe_xNi_y was x Fe and y Ni, while similarly for Fe_xPd_y the input was x Fe and y Pd . However, this prediction quality is comparable with the other techniques for modeling multi-component systems without need of describing the atomic interactions, but with more applicability by not requiring an input Hamiltonian, and is sufficient for representing the significant features of the DOS curve. Additionally, this level of accuracy is particularly notable given the limited amount of input information needed. As

most elemental DOS are known, this approach then allows us to model DOS of any chemistry and stoichiometry.

In these results, the accuracy of the model is comparable to that for the training systems, indicating that our model is not over-fitting the data. The crystal structures for these systems were not input into the model, but we still capture the interactions accurately. For FeNi and FePd, the crystal structure type is $L1_0$, while for FeX_3 and Fe_3X (X=Pd, Ni), the crystal structure type is $L1_2$. Capturing the general shape of the DOS curves indicates that ANN is able to extract the electronic interactions from the elemental DOS, and is able to represent the form of these electronic interactions in multi-component systems.

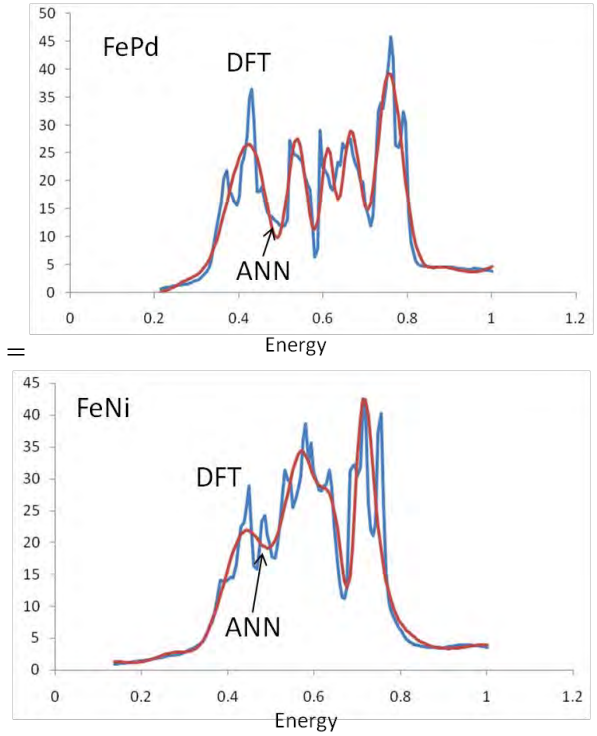

Figure 15. Testing of DOS modeled for FePd and FeNi using the trained ANN. These two chemistries were not included in the development of the ANN model, and serve as validation sets of the approach. The accuracy of the test DOS is comparable with the training DOS, indicating that we have avoided an over-fitting of the data, and the model is applicable for other stoichiometries of the elements.

Using the developed logic, the bulk modulus of the training and test systems were predicted (Figure 16). From this figure, we find that the logic is capable of predicting bulk modulus from the DOS spectra with high accuracy. Additionally, the model predicts bulk modulus well for both the training and test systems, indicating that our model is not over-fitting the training data. The input for the test systems was only ANN modeled

DOS, with no input of bulk modulus. The accuracy of this result validates that the level of detail of the ANN model is sufficient for describing the alloys. This work, combined with the work on charge density topology, shows the value of informatics analysis of *ab initio* calculated data.

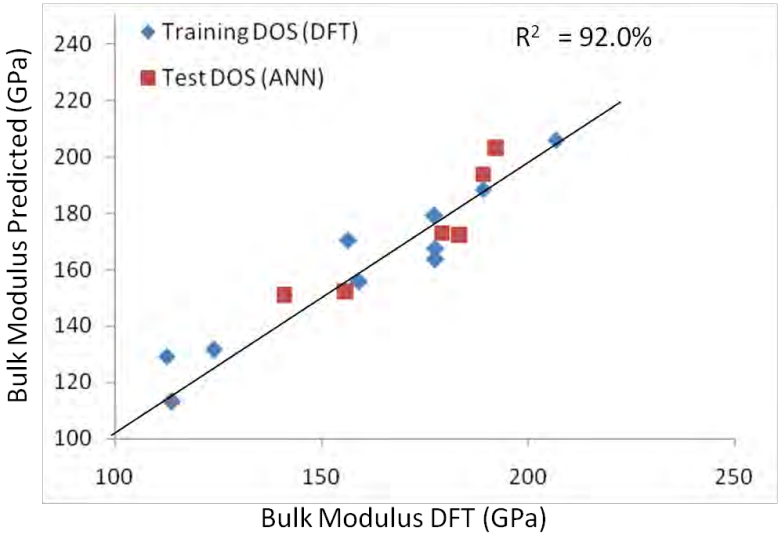

Figure 16. The result of the approach for predicting bulk modulus from an input of alloy DOS spectra. The diamonds correspond to DOS calculated by DFT while the squares correspond to DOS modeled via ANN. The bulk modulus of the training systems was used to train the model, while the bulk modulus of the test systems was not used in any form in developing the model. The accuracy of the results demonstrates that bulk modulus is clearly represented within the DOS spectra, and that it can be quantitatively extracted via statistical learning. Additionally, the accuracy of the bulk modulus predicted for the test systems indicates that the ANN approach for modeling DOS is sufficiently detailed and accurate.

Statistics for September 2012 – August 2013

Publications

1. **Informatics for Materials Science and Engineering**: editor Krishna Rajan ; Elsevier ISBN: 9780123943996 (2013)

2. M.E. Eberhart and T.E. Jones**,** "The two faces of chemistry: can they be reconciled?", Foundations of Chemistry, **15**, 277-285 (2013)

3. S. Ganguly, C.S. Kong, S.R. Broderick, K. Rajan. "Informatics Based Uncertainty Quantification in the Design of Inorganic Scintillators", *Materials and Manufacturing Processes*, **28**, 726-732 (2013)

4. E.W. Bucholz, C.S. Kong, K.R. Marchman, W.G. Sawyer, S.R. Phillpot, S.B. Sinnott, K. Rajan, "Data-Driven Model of Friction Coefficient via Informatics Methods", *Tribology Letters*, **47**, 211-221 (2012)

5. M.E. Eberhart, T.E. Jones, "Cauchy pressure and the generalized bonding model for nonmagnetic bcc transition metals", *Physical Review B,* **86**, 134106, (2012)

6. T.E. Jones, M.E. Eberhart, S. Imally, C. Mackey, G.B. Olson, "Better Alloys with Quantum Design", *Physical Review Letters*, **109**, 125506, (2012).

7. R. Zhang, S.R. Broderick, S. Srinivasan, K. Rajan. "Dynamic Mapping of the Modulus Landscape for Spinel Nitrides through Statistical Learning", *New Journal of Physics* (Submitted)

8. J. Miorelli, S. Morgenstern, T. Wilson, T.E. Jones, and M.E. Eberhart, "Advances in Conceptual Density Functional Theory", *Chemistry European Journal* (Submitted)

9. M.E. Eberhart, "Identifying Chemical Functionalities in Metals and Alloys", *Science* (Submitted)

10. T.E. Jones, J. Miorelli, M.E. Eberhart, "Reactive Cluster Model of Metallic Glasses", *Journal of Chemical Physics* (Submitted)

11. C.S. Kong, S.R. Broderick, C. Loyola, T.J. Jones, M.E. Eberhart, K. Rajan, "Informatics-Defined Quantitative Charge Density - Elastic Behavior Relationship", Physical Review B, To be submitted December 2013

12. M.E. Eberhart, "Cauchy pressure and the generalized bonding model for nonmagnetic fcc transition metals", *Physical Review B*, To be submitted December 2013

13. S.R. Broderick, M.E. Eberhart, K. Rajan, "Why do Transition Metals Form in their Crystal Structures? Hume-Rothery Revisited", (In Preparation)

14. S.R. Broderick, T.J. Jones, M.E. Eberhart, K. Rajan, "Informatics-based Electronic Design via Modeling Charge Density Topology ", (In Preparation)

15. S.R. Broderick, S. Ganguly, K. Rajan, "Data Mining Density of States Spectra: A "Genomics" Paradigm for Alloy Property Prediction", (In preparation)

16. S.R. Broderick, K. Rajan, "Modeling of Deformation Mechanisms of Al Alloys by Data Mining Density of States Spectra", (In preparation)

Presentations

Krishna Rajan, Iowa State University:

1. Discovering Materials Science through Data Science
   Department of Materials Science and Engineering
   Carnegie Mellon University
   Pittsburgh PA. September 14th 2012

2. Informatics for Discovering the Materials Genome
   Scientific Discovery Initiative Seminar Series
   Pacific Northwest National Laboratory
   Richland WA. September 19th 2012

3. Expanding the Design Limits in Materials via Data Mining
   Symposium on Data Science Approaches for Mechanics of Materials
   22nd International Workshop on Computational Mechanics of Materials
   Baltimore Sept. 24-26th 2012

4. Informatics for the Inverse Design of Materials
   49th Annual Society of Engineering Science Meeting
   Atlanta GA; October 10-12, 2012

5. "omics" for Materials Science via Informatics
   Symposium on Materials Informatics
   Materials Research Society Fall 2012 meeting
   Boston MA; Nov. 26th-30th 2012

6. Materials Co-Design for Translational Breakthroughs in Technology
   Workshop on New and Novel Processes that are on the Verge of Industrial Modernization - Defense Materials Manufacturing and Infrastructure
   National Academy of Sciences
   Washington DC ; December 5th 2012,

7. Grand Challenges in Computational Materials Design Workshop
   North Carolina State University
   Raleigh, NC; Jan. 15-16th 201

8. Mapping the Materials Genome Landscape
   1st International Conference on Molecular and Materials Informatics
   Melbourne, Australia
   February 4-6, 2013

9. Mapping the Electronic Structure Landscape for Materials Discovery
   German Physical Society (DPG) meeting
   Regenseberg, Germany
   March 15th 2013

10. Enabling ICSME through Informatics and Big Data
    Air Force Research Laboratory- Materials and Manufacturing Directorate
    Wright Patterson Air Force Base
    Dayton OH ; March 20th 2013

11. Informatics Aided Discovery of Energy Materials
    2013 Kentucky Workshop on Renewable Energy and Energy Efficiency
    Louisville KY ; March 25th 2013

12. Discovering Classfiers in Materials Science through Statistical Learning
    Workshop on Machine Learning and Materials Science
    Santa Fe Institute
    Santa Fe , NM - April 3rd 2013

13. Nanoinformatics for Materials Chemistry
    NSF Workshop - Cyberinfrastructure for Environmental Nanoinformatics
    Center for Environmental Implications of Nanotechnology –UCLA
    Los Angeles CA- May 7th 2013

14. Informatics for Ceramic Crystal Chemistry
    Ceramics by Genome Symposium
    10th Pacific Rim Conference on Ceramic and Glass Technology
    San Diego, CA
    June 6th 2013

15. Statistical Learning Guided Design of Materials

Fritz Haber Institute – Theory Group
Berlin , Germany
June 17th 2013

16. Developing Property Maps to Guide Materials Design via Statistical Learning
Summer Research Group Meeting – Materials by Design
Los Alamos National Laboratory
July 17, 2013

Students and Associates

Iowa State University

Claudia Loyola – Post-doctoral associate

Scott Broderick – Research assistant professor

John Graham – BS/MS Student, Department of Materials Science and Engineering

Colorado School of Mines

Jonathan Miorelli -- Ph.D. student, Department of Chemistry

Samantha Morgenstern -- Ph.D. student, Department of Chemistry

Tim Wilson – Undergraduate student, Department of Chemical and Biological Engineering